Available online at www.sciencedirect.com
ScienceDirect
Journal of Computational Physics 219 (2006) 163–171
JOURNAL OF COMPUTATIONAL PHYSICS
www.elsevier.com/locate/jcp

An alternative discretization and solution procedure for the dual phase-lag equation

J.M. McDonough [a,b,*], I. Kunadian [a], R.R. Kumar [a], T. Yang [c]

[a] Department of Mechanical Engineering, University of Kentucky, 151 RGAN Building, Lexington, Kentucky 40506-0503, USA
[b] Department of Mathematics, University of Kentucky, 151 RGAN Building, Lexington, Kentucky 40506-0503, USA
[c] Convergent Thinking, LLC, Madison, WI 53719, USA

Received 11 August 2005; received in revised form 17 January 2006; accepted 18 March 2006
Available online 2 June 2006

Abstract

We describe an alternative numerical treatment of the dual phase-lag equation often used to account for microscale, short-time heat transport. The approach consists of an undecomposed formulation of the partial differential equation resulting from Taylor expansion with respect to lag times of the original delay partial differential equation. Trapezoidal integration in time and centered differencing in space provide an accurate discretization, as demonstrated by comparisons with analytical and experimental results in one dimension, and via grid-function convergence tests in three dimensions. For relatively fine 3-D grids the approach is approximately six times faster than a standard explicit scheme and nearly three times faster than an implicit method employing conjugate gradient iteration at each time step.

Keywords: Microscale; Heat transport equation; Phase lags; Delay equations; von Neumann stability; Truncation error; Douglas–Gunn time splitting

1. Introduction

Fourier's law predicts infinite-velocity propagation of thermal disturbances, implying that a thermal perturbation applied at any location in a solid medium can be sensed immediately anywhere else in the medium (violating precepts of special relativity). Associated with this is the fact that the parabolic character of the heat equation obtained from Fourier's law implies that heat flow starts (stops) simultaneously with appearance (disappearance) of a temperature gradient, thus violating the causality principle which states that two causally correlated events cannot happen at the same time; rather, the cause must precede the effect, as noted by Cimmelli [1]. In order to ensure finite propagation of thermal disturbances a hyperbolic heat conduction equation (HHCE) was proposed at least as early as the studies of Luikov [2] and Baumeister and Hamil [3]. We remark

* Corresponding author. Tel.: +1 859 257 6336; fax: +1 859 257 3304.
E-mail addresses: jmmcd@uky.edu (J.M. McDonough), ikuna0@engr.uky.edu (I. Kunadian), rrkuma0@engr.uky.edu (R.R. Kumar), tlyang@c-think.com (T. Yang).

0021-9991/$ - see front matter © 2006 Elsevier Inc. All rights reserved.
doi:10.1016/j.jcp.2006.03.023

that this equation is of the same form as that termed the "telegraph equation" in the mathematics literature (see essentially any intermediate PDE text). More recently, it has been shown that in certain situations HHCEs violate the second law of thermodynamics resulting in physically unrealistic temperature distributions such as temperature overshoot phenomena observed in a slab subject to a sudden temperature rise on its boundaries (see, e.g. Taitel [4]). Also, since the classical Fourier and hyperbolic models neglect thermalization time (time for electrons and lattice to reach thermal equilibrium) and relaxation time of the electrons, their applicability to very short-pulse laser heating becomes questionable, as noted by Qiu and Tien [5,6] and Qiu et al. [7].

Kagnov et al. [8] were among the first to theoretically evaluate the microscopic (thermal) exchange between electrons and the lattice. Following this, Anisimov et al. [9] proposed a two-step model to describe electron and lattice temperatures, T_e and T_l, respectively, during the short-pulse laser heating of metals. Later, Qiu and Tien [5,6] rigorously derived the hyperbolic two-step model from the Boltzmann transport equation for electrons. They then numerically solved the model equations for the case of a 96 fs duration laser pulse irradiating a thin film of thickness 0.1 μm. The predicted temperature change of the electron gas during the picosecond transient agreed well with experimental data, supporting validity of the hyperbolic two-step model for describing heat transfer mechanisms during short-pulse laser heating of metals.

Even though this microscopic model works quite well at small scales, when investigating macroscopic effects a different model might be desirable. Tzou proposed the dual phase-lag (DPL) model [10–13] that reduces to diffusion, thermal wave, the phonon–electron interaction [5,6], and the pure phonon scattering [14] models as values of model parameters τ_q and τ_T are changed, permitting coverage of a wide range of physical responses, from microscopic to macroscopic scales, in both space and time, ostensibly with a single formulation in terms of a single temperature.

Zhou et al. [15] argue that the DPL equation is only a relaxed mathematical representation with no sound physical interpretation attached to it. In particular, the temperature distribution predicted by the DPL model does not correspond to either the electron temperature T_e or the lattice temperature T_l. Thus, the objective of the present paper is not to attempt validation of the DPL model as a description of physics, but rather to present a method for treating equations such as this (involving lagging and mixed derivatives) and provide a procedure to efficiently solve them in the context of a relatively simple (single-temperature) formulation.

In recent years, various numerical methods have been investigated for solving the DPL equation. Most early numerical studies involved only the 1-D equation, often using explicit discretization in time. Recent studies have begun to consider 2-D and 3-D DPL equations, with implicit discretizations. Dai and Nassar [16,17] have developed an implicit finite-difference approach in which the DPL equation is split into a system of two equations; the individual equations are discretized using the Crank–Nicolson scheme and solved sequentially. The method has been generalized to 3-D by Dai and Nassar [18–20] and applied to the case of heating a rectangular thin film with thickness at the sub-micron scale.

Zhang and Zhao [21,22] have employed the iterative techniques Gauss–Seidel, successive overrelaxation (SOR) with optimal overrelaxation parameters, conjugate gradient (CG), and preconditioned conjugate gradient (PCG) to solve the 3-D discrete DPL equation with Dirichlet boundary conditions. In contrast, applying Neumann boundary conditions (as often needed for heat transfer problems) can result in non-symmetric seven-band (in 3-D) positive semi-definite matrices that can be unsuitable for treatment with iterative methods of the nature of CG and PCG, suggesting that other approaches should also be considered.

The purpose of the present paper is to provide a formulation based on a single 1-D DPL equation (in contrast to the usual two coupled equations) solved via trapezoidal integration. The numerical technique will be extended to three dimensions using a Douglas–Gunn time-splitting method in δ form, and efficiency of this approach will be assessed via comparisons with other current solution procedures reported in the recent literature. Comparisons of 1-D results with both analytical and experimental results are presented, and 3-D simulations are provided for a case of femtosecond pulsed-laser heating of a thin gold film.

2. Analysis

Mathematically, the dual phase-lag concept can be represented as in [11] with heat flux expressed as

$$\boldsymbol{q}(\boldsymbol{x}, t + \tau_q) = -\lambda \nabla T(\boldsymbol{x}, t + \tau_T), \tag{1}$$

where τ_T is the "phase lag" of the temperature gradient, and τ_q is the corresponding lag of the heat flux vector. Here λ represents thermal conductivity and $\boldsymbol{x}$ is a spatial location. There are three characteristic times involved in the dual phase-lag model: the instant of time $t+\tau_T$ at which the temperature gradient is established across a material volume, the time $t+\tau_q$ for the onset of heat flow, and time t for the transient heat transport.

Application of the first law of thermodynamics in the usual way leads to

$$\frac{\partial T}{\partial t}(\boldsymbol{x}, t+\tau_q) = \alpha \Delta T(\boldsymbol{x}, t+\tau_T), \tag{2}$$

which is a delay partial differential equation with two separate delays. Here, α is thermal diffusivity and Δ is the Laplace operator in an appropriate coordinate system. In this form the mathematical problem is nearly intractable, both analytically and numerically. But if we assume T is sufficiently smooth in time we can expand it in Taylor series about t, separately, with respect to each of τ_q and τ_T:

$$T(\boldsymbol{x}, t+\tau_q) = T(\boldsymbol{x}, t) + \frac{\partial T}{\partial t}(\boldsymbol{x}, t)\tau_q + \cdots$$

and

$$T(\boldsymbol{x}, t+\tau_T) = T(\boldsymbol{x}, t) + \frac{\partial T}{\partial t}(\boldsymbol{x}, t)\tau_T + \cdots$$

where we have neglected all higher-order terms. Clearly, if higher-order derivatives remain bounded we should expect this approximation to be at least qualitatively accurate because τ_T and τ_q are expected to be small. Substitution of these expressions into (2) leads to

$$\tau_q \frac{\partial^2 T}{\partial t^2} + \frac{\partial T}{\partial t} - \tau_T \alpha \frac{\partial(\Delta T)}{\partial t} = \alpha \Delta T + \frac{\alpha}{\lambda}\left(S + \tau_q \frac{\partial S}{\partial t}\right), \tag{3}$$

in which we have added a source term of a form corresponding to pulsed-laser irradiation. Details of the function S used in the present study will be given below.

It should be clear that analysis of (3) is far more straightforward than that of Eq. (2), despite presence of the third-order mixed derivative term, because there are now no delays. In particular, complete well-posed problems for the HHCE are also well posed for (3), at least with respect to required data. Furthermore, we see that when $\tau_T = 0$ the HHCE is recovered, and if both τ_T and τ_q are zero the usual parabolic heat equation results.

As was hinted above, it has been customary to decompose (3) as a system of two equations containing no mixed derivative. There are at least a couple versions of this, and we refer the reader to [20] for one example. But such decompositions rely on constancy of τ_q and τ_T, and while this is not an unreasonable expectation it is at least of interest to seek a solution approach not depending on this requirement. Loss of this required constancy could occur (spatially) for non-homogeneous materials, and, in general, if τ_q and τ_T depend on T, leading to nonlinearities. Directly solving Eq. (3), as we will describe in the sequel, provides a way to handle these situations although this is not the focus of the present work.

We begin by applying trapezoidal integration to Eq. (3) to obtain

$$\begin{aligned} &T^{n+1} - T^n + \tau_q\left[\left(\frac{\partial T}{\partial t}\right)^{n+1} - \left(\frac{\partial T}{\partial t}\right)^{n}\right] - \tau_T \alpha\left(\Delta T^{n+1} - \Delta T^n\right) \\ &\quad = \alpha\frac{k}{2}\left(\Delta T^{n+1} + \Delta T^n\right) + \frac{\alpha}{\lambda}\frac{k}{2}\left(S^{n+1} + S^n\right) + \frac{\alpha}{\lambda}\tau_q\left(S^{n+1} - S^n\right) \end{aligned} \tag{4}$$

with k denoting the time step size (Δt) and superscripts indicating time levels.

We apply a second-order backward difference to discretize the time derivative at time level $n+1$ and a centered difference for the time derivative at n. The second-order derivatives in space are approximated using a centered-difference scheme: thus,

$$\left(\frac{\partial T}{\partial t}\right)^{n+1}_{\boldsymbol{m}} \cong \frac{1}{2k}\left[3T^{n+1}_{\boldsymbol{m}} - 4T^{n}_{\boldsymbol{m}} + T^{n-1}_{\boldsymbol{m}}\right], \tag{5a}$$

$$\left(\frac{\partial T}{\partial t}\right)^{n}_{\boldsymbol{m}} \cong \frac{1}{2k}\left[T^{n+1}_{\boldsymbol{m}} - T^{n-1}_{\boldsymbol{m}}\right], \tag{5b}$$

$$\left(\frac{\partial^2 T}{\partial x^2}\right)^{n}_{\boldsymbol{m}} \cong \frac{1}{h^2}\left[T_{\boldsymbol{m}+1} - 2T_{\boldsymbol{m}} + T_{\boldsymbol{m}-1}\right], \tag{5c}$$

where subscripts represent spatial multi indices, and we have written these approximations without their associated truncation errors. The last of these holds for both time levels included in Eq. (4) and in each of the appropriate spatial directions. In Eq. (5c) $h \equiv (b-a)/(N_x - 1)$ is the spatial step size for a 1-D spatial domain $\Omega \equiv [a,b]$ discretized with N_x uniformly-spaced grid points. The form of appropriate expressions for higher dimensions is obvious. These approximations render the numerical scheme globally first-order accurate in time and second-order accurate in space.

We have analyzed stability of the above scheme via a von Neumann analysis (to be reported elsewhere), but because Eq. (4) becomes a three-level difference approximation upon introduction of (5a) and (5b), the von Neumann condition supplies only a necessary (but not sufficient) stability criterion in general. Thus, we have performed numerous computations with a wide range of values of h,k and combinations of the physical parameters chosen so as to include both hyperbolic and parabolic cases of the DPL equation, and for values of k/h^2 as high as 10^6. We have been unable to find any combinations that lead to long-time blowup of solutions. Thus, unconditional stability appears to be likely, but it has not been proven.

3. Efficient solution of 3-D DPL equation

Recent work in both 2-D and 3-D has often employed iterative methods to solve the algebraic systems arising at each discrete time step; this can be quite inefficient, especially when very fine spatial grids are being used. Here, we will utilize a very old approach that has been widely employed in computational fluid dynamics to efficiently treat the 3-D problem, but we note that this technique is basically not applicable when unstructured meshes are used.

The combination of Eqs. (4) and (5) can be expressed in the standard form of a $M+2$-level difference equation to which the Douglas–Gunn time-splitting formalism [23] can be directly applied; namely,

$$(\boldsymbol{I} + \boldsymbol{A}^{n+1})T^{n+1} + \sum_{m=0}^{M} \boldsymbol{B}^{n}_{m} T^{n-m} = s^{n} \tag{6}$$

with $M = 1$ in the case of the three-level scheme being considered here. Bold symbols denote $N \times N$ matrices with $N \equiv N_x N_y N_z$, the product of the number of grid points in each coordinate direction, and $\boldsymbol{I}$ is the identity matrix. This equation holds at all points of the discrete solution domain except at boundaries, where some modifications are necessary. We also remark that in the cases being treated herein the temporal indexing of matrices is merely formal.

The matrix $\boldsymbol{A}^{n+1}$ consists of terms arising from spatial discretization at time level $n+1$; viz.,

$$\boldsymbol{A}^{n+1} = \sum_{\ell=1}^{N_s} \boldsymbol{A}^{n+1}_{\ell}, \tag{7}$$

where N_s is in general the number of split steps (which in the present case is the number of spatial dimensions of the solution domain). Also, the $\boldsymbol{B}$ matrices are constructed as follows:

$$\boldsymbol{B}^{n}_{0} = \boldsymbol{A}^{n} - \frac{2\tau_q/k}{1+\tau_q/k}\boldsymbol{I}, \quad \boldsymbol{B}^{n}_{1} = \frac{\tau_q/k}{1+\tau_q/k}\boldsymbol{I}. \tag{8}$$

In the first of these the matrix $\boldsymbol{A}^{n}$ arises from spatial discretization of the Laplacian at time level n.

Formal time splitting of this, followed by some rearrangement, leads to the so-called δ form of Douglas–Gunn time splitting:

Table 1
Performance comparison of different numerical methods for solving the discretized 3-D DPL equation

Numerical techniques	Total required CPU time (s)			
	$N = 21^3$	$N = 41^3$	$N = 51^3$	$N = 101^3$
Explicit scheme	4.88	147.62	450.26	7920.00
Conjugate gradient	12.33	124.83	270.30	3614.69
δ-form Douglas–Gunn	8.54	70.50	140.92	1344.40

$$(\boldsymbol{I} + \boldsymbol{A}_1)\delta T^{(1)} = s^n - (\boldsymbol{I} + \boldsymbol{A})T^n - \sum_{m=0}^{1} \boldsymbol{B}_m T^{n-m},$$
$$(\boldsymbol{I} + \boldsymbol{A}_\ell)\delta T^{(\ell)} = \delta T^{(\ell-1)}, \quad \ell = 2, \ldots, N_s,$$

where $\delta T^{(\ell)} \equiv T^{(\ell)} - T^n \Rightarrow T^{n+1} = T^n + \delta T^{(N_s)}$.

In this form we recognize that the right-hand side of the first equation is the original discrete equation evaluated at time level n, so the amount of required arithmetic is $\mathcal{O}(N)$ – essentially that required for an explicit method. Then there are N_s matrix–vector solves to be performed. In the present case, each of these involves a tridiagonal matrix, which also leads to $\mathcal{O}(N)$ arithmetic per solve. For the ℓth split step this takes the form

$$C_1^{(\ell)}\delta T_{\boldsymbol{i}-1}^{(\ell)} + C_2^{(\ell)}\delta T_{\boldsymbol{i}}^{(\ell)} + C_1^{(\ell)}\delta T_{\boldsymbol{i}+1}^{(\ell)} = \delta T_{\boldsymbol{i}}^{(\ell-1)}$$

with the coefficients defined as

$$C_1^{(\ell)} \equiv -\frac{\tau_T + k/2}{h_\ell^2(1 + \tau_q/k)}, \quad C_2^{(\ell)} \equiv 1 + \frac{2(\tau_T + k/2)}{h_\ell^2(1 + \tau_q/k)}$$

and $\boldsymbol{i}$ denotes a generic multi index for (3-D) gridpoint notation with shifts only in the ℓth slot. Furthermore, we associate h_x with $\ell = 1$, i.e., $h_1 = h_x$, etc.

It is worthwhile at this point to recall some of the features of Douglas–Gunn time splitting presented in [23]. First, it is proven in that work that up through second-order temporal accuracy, the split scheme retains the accuracy of the unsplit scheme. Second, it is also shown that stability of the unsplit scheme is inherited by the split scheme. Finally, we remark that these favorable properties of the Douglas–Gunn split scheme are proven in [23] under quite stringent conditions associated with solution regularity and commutativity of the various matrices appearing in Eqs. (7) and (8). But it is usually found in practice that these requirements can be relaxed significantly without affecting behavior of the method.

We quantify computational efficiency with data presented in Table 1 which contains a sampling of results given by Kunadian et al. [24]. Table 1 shows CPU time in seconds required to complete an entire simulation to a fixed final time for explicit, conjugate gradient and δ-form Douglas–Gunn time-splitting methods using different values of number of grid points $N = N_x N_y N_z$. The spatial domain consists of a cube with uniform grid spacing, and equal number of grid points, in each of the three separate directions.

From Table 1 we can observe that for extremely coarse grids the explicit method consumes less CPU time than that required by the other numerical techniques, but as the spatial resolution is refined the implicit methods perform better than the simple forward-Euler/centered-difference explicit method employed in this research due to the small time steps required for stability of the latter. The δ-form Douglas–Gunn time-splitting used in the present study consumes the least CPU time of the three methods considered; moreover, its degree of superiority increases with spatial resolution, and it is highly parallelizable. Further comparisons of this sort over a wide range of currently-used methods are forthcoming in a paper by Kumar et al. [25] where it is shown that for high-resolution calculations on grids having greater than a million grid points, time splitting is significantly more efficient for time-dependent problems than any iterative technique.

4. Computed results for specific problems

In this section we provide some representative results associated with simulating physical problems of the sort for which the DPL equation was originally intended. In the first subsection calculations corresponding to

a 1-D model of laser heating of a thin gold film are presented and compared with analogous analytical and experimental results, and in a second subsection simulations from a 3-D model problem are presented.

4.1. 1-D laser heating of gold film

The equation solved in this case is Eq. (3) with the Laplacian replaced by $\partial^2/\partial x^2$ and the right-hand side forcing constructed from

$$S(x,t) = 0.94J\left[\frac{1-R}{t_p\delta}\right]\exp\left(-\frac{x}{\delta}-\frac{1.992\mid t-2t_p\mid}{t_p}\right), \tag{9}$$

where laser fluence $J = 13.7\ \mathrm{J/m^2}$, and $t_p = 96$ fs; penetration depth is $\delta = 15.3$ nm, and reflectivity is $R = 0.93$, as presented in [26]. The initial conditions are $T \equiv 0$ and $\partial T/\partial t \equiv 0$ on Ω; no-flux boundary conditions are employed at both ends of the interval. We note that differentiation of S as required in (3) poses a mild difficulty due to the form of (9), but this does not create a major problem since the Heaviside function is in $L^1(\Omega)$ for bounded Ω. In this problem the spatial domain Ω is the film thickness (0.1 μm). The problem is discretized with $N_x = 1001$ points, and a time step $k = 1.25\times10^{-14}$ s was used. Grid-function convergence tests indicate that this provides sufficient resolution, and this is confirmed by comparisons with analytical results shown in Fig. 1.

Fig. 1 presents a comparison between the numerical, analytical [26] and experimental results of Brorson et al. [27] and Qiu and Tien [5,6] corresponding to the front surface transient response for a 0.1 μm thick gold film. Thermal properties of the material ($\alpha = 1.2\times10^{-4}\ \mathrm{m^2\,s^{-1}}$, $\lambda = 315\ \mathrm{W\,m^{-1}\,K^{-1}}$, $\tau_T = 90$ ps, $\tau_q = 8.5$ ps) are assumed to be constant. The temperature change has been normalized by the maximum value that occurs during the short-time transient. Results from the present numerical scheme compare nearly perfectly with analytical results (confirming adequacy of the discretization step sizes) and reasonably well with experimental results, while the HHCE and parabolic models, which neglect the microstructural interaction effects during the short-time transient, overestimate temperature during most of the transient response, as shown in Fig. 1.

4.2. 3-D pulsed-laser heating of gold film

For this problem the full 3-D form of Eq. (3) is employed with a source term constructed from S given as

$$S(\boldsymbol{r},t) = 0.94J\left[\frac{1-R}{t_p\delta}\right]\exp\left(-\frac{\left(x-\frac{L_x}{2}\right)^2+\left(y-\frac{L_y}{2}\right)^2}{2r_0^2}-\frac{z}{\delta}-\frac{1.992|t-2t_p|}{t_p}\right), \tag{10}$$

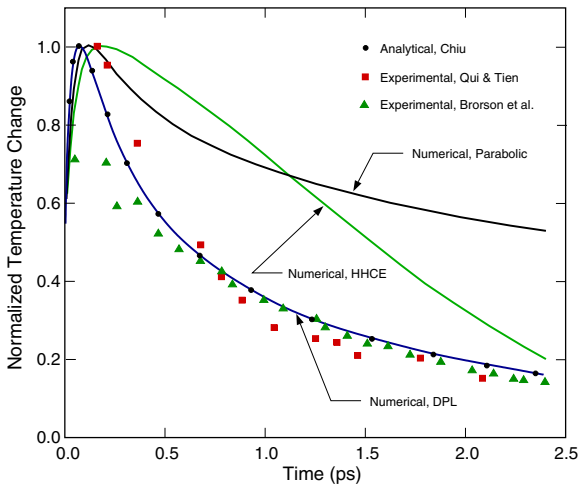

Fig. 1. Front surface transient response for a 0.1 μm gold film. Comparison among numerical, analytical and experimental results.

where L_x and L_y are the length and width of the metal film, respectively, and r_0 is radius of the laser beam oriented in the z-direction. Initial and boundary conditions are the same as in the 1-D case but with the former imposed on the whole volume Ω of the problem domain and the latter now applied over the entire surface $\partial\Omega$. This domain is again a gold film of thickness 0.1 μm but now with lateral extent 0.5 μm × 0.5 μm. The spatial discretization was constructed on a grid of $101 \times 101 \times 21$ uniformly-spaced points in each of the three directions and utilizing times steps of 1×10^{-14} s. As noted in Section 2, Eq. (3) acquires DPL, HHCE and parabolic character according to the values selected for τ_T and τ_q. Here, we have used $\tau_T = 90$ ps, $\tau_q = 8.5$ ps $\Rightarrow$ DPL model; $\tau_T = \tau_q = 0 \Rightarrow$ parabolic model and $\tau_q = 8.5$ ps, $\tau_T = 0 \Rightarrow$ hyperbolic model. Thus, we are able to employ the same code for all calculations.

Fig. 2 displays a comparison (at two different times) of transient temperature distribution caused by a pulsating laser beam of 200 nm diameter heating the top surface of the gold film at various locations near its corners (with movement from one corner to the next successive one in a counter-clockwise direction) every 0.3 ps, as predicted by DPL, hyperbolic and parabolic heat conduction models. (Bright red represents the highest temperatures, and deep blue corresponds to the lowest ones.) Fig. 2 shows that HHCE and parabolic diffusion models predict a higher temperature over a wider area near the film's surface in the heat-affected zone than does the DPL model, but the penetration depth is much shallower. The heat-affected zone is significantly deeper for the DPL model than for the other models due to the microstructural interaction effect incorporated in the formulation of this model. Furthermore, discrepancies between DPL and the other two models grow significantly with time, as is evident from part (b) of Fig. 2.

We have been unable to acquire 3-D experimental data with which to make quantitative comparisons with these simulations. However, Table 2 presents results of grid-function convergence tests that indicate overall validity of the implementation in the sense that theoretical convergence rates are closely matched by the numerical results. In particular, it is easy to show that the dominant truncation error of our discretization is $\sim O(h_x^2 + h_y^2 + h_z^2 + k)$. This implies that if we were to hold the time step size k fixed and reduced the spatial step sizes uniformly, the error would decrease by the factor r^{-q}, where r is the space step size ratio, and q is the power on the dominant truncation error. In the present case, if we halve the grid spacing, the error should decrease by a factor of four. To simultaneously account for the temporal error it is thus convenient to reduce time step sizes by a factor of four as grid spacing is halved.

We have used this procedure at three different spatial grid points, recording results from each at a different time during the simulations, and calculated q from the numerical results. These results are presented in Table 2.

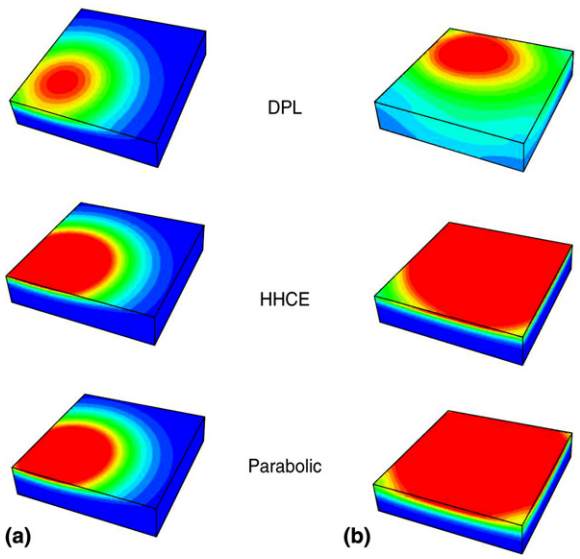

Fig. 2. Temperature distribution in gold film predicted by DPL, hyperbolic and parabolic heat conduction models: (a) at 0.31 ps; (b) at 2.18 ps.

Table 2
Grid-function convergence for time-split DPL equation

Space-time points		Temperature (K)			
Spatial location	Time (ps)	Coarse	Medium	Fine	q
$x = y = 250$ nm, $z = 1$ nm	2.5	301.8060	301.8030	301.8023	2.10
$x = y = 250$ nm, $z = 50$ nm	3.0	301.8245	301.8175	301.8157	1.96
$x = y = 250$ nm, $z = 100$ nm	3.5	301.7797	301.7732	301.7716	2.02

This sequence of calculations was started with step sizes $h_x = h_y = 25$ nm, $h_z = 5$ nm and $k = 10$ fs. Temperature values in Kelvins are shown in the third column of Table 2 (corresponding to "coarse" gridding) at three combinations of spatial location and time: (i) $x = y = 250$ nm, $z = 1$ nm, $t = 2.5$ ps; (ii) same x, y, with $z = 50$ nm, $t = 3$ ps; (iii) same x, y, $z = 100$ nm, $t = 3.5$ ps. Columns four and five show results at the same set of space-time points, but with grid spacing halved and reduced by a factor of four, respectively, and with time step sizes correspondingly reduced by factors of four and 16. The final column displays values of q calculated from these data. These are uniformly quite close to the theoretical value $q = 2$, suggesting that even results from the coarsest grid are reasonably accurate.

5. Summary and conclusions

We began by deriving the DPL equation by simple Taylor expansion applied to a much more (mathematically-) complicated delay PDE. We then developed a strongly stable implicit finite-difference scheme of Crank–Nicolson type for solving the DPL equation, without appealing to the standard decomposition typically employed. The method is first-order accurate in time (despite its trapezoidal integration origins) and second order in space; reported 1-D numerical experiments suggest, but of course do not prove, unconditional stability.

Results from 1-D calculations were shown to be in excellent agreement with analytical results (obtainable only in 1-D) and in significantly better agreement with experiment than either HHCE or classical parabolic heat equation results. The 3-D DPL equation was solved using a δ-form Douglas–Gunn time-splitting method. This approach was shown to outperform both explicit time stepping and a conjugate gradient iterative procedure in terms of computation time required to complete a simulation. Finally, we presented limited computed results for a realistic 3-D physical problem (for which there are currently no available experimental data) and demonstrated grid-function convergence of computed results to validate this case.

The treatment we have employed to arrive at the DPL equation is quite simple and may have applicability more generally for other delay PDEs. The un-decomposed solution formalism employed here has the advantage of direct application to variable-coefficient PDEs. Its only disadvantage is the need to numerically treat a third-order mixed (space and time) derivative and a second-order time derivative. Use of Douglas–Gunn time splitting in the solution of the multi-dimensional DPL equation appears to be nearly optimal, especially as problem size (number of spatial grid points and/or required number of time steps) becomes large.

References

[1] V.A. Cimmelli, Boundary conditions for diffusive hyperbolic systems in non-equilibrium thermodynamics, Technische Mechanik (2002) 181, Band 22, Heft 3.
[2] A.V. Luikov, Application of irreversible thermodynamics methods to investigation of heat and mass transfer, International Journal of Heat and Mass Transfer 9 (1966) 139.
[3] K.J. Baumeister, T.D. Hamil, Hyperbolic heat conduction equation: a solution for the semi-infinite body problem, ASME Journal of Heat Transfer 91 (1969) 543.
[4] Y. Taitel, On the parabolic, hyperbolic and discrete formulation of the heat conduction equation, International Journal of Heat and Mass Transfer 15 (1972) 369.
[5] T.Q. Qiu, C.L. Tien, Short-pulse laser heating of metals, International Journal of Heat and Mass Transfer 35 (1972) 719.
[6] T.Q. Qiu, C.L. Tien, Heat transfer mechanisms during short-pulse laser heating of metals, ASME Journal of Heat Transfer 115 (1993) 835.
[7] T.Q. Qiu, T. Juhasz, C. Suarez, W.E. Bron, C.L. Tien, Femtosecond laser heating of multi-layered metals – II. Experiments, International Journal of Heat and Mass Transfer 37 (1994) 2799.
[8] M.I. Kagnov, I.M. Lifshitz, M.V. Tanatarov, Relaxation between electrons and crystalline lattices, Soviet Physics JETP 4 (1957) 173.

[9] S.I. Anisimov, B.L. Kapeliovich, T.L. Perel'man, Electron emission from metal surfaces exposed to ultrashort laser pulses, Soviet Physics JETP 39 (1974) 375.
[10] D.Y. Tzou, Macro-to-Microscale Heat Transfer: The Lagging Behavior, Taylor & Francis, Washington, DC, 1996.
[11] D.Y. Tzou, A unified approach for heat conduction from macro-to-micro scales, ASME Journal of Heat Transfer 117 (1995) 8.
[12] D.Y. Tzou, The generalized lagging response in small-scale and high-rate heating, International Journal of Heat and Mass Transfer 38 (1995) 3231.
[13] D.Y. Tzou, Experimental support for lagging behavior in heat propagation, Journal of Thermophysics and Heat Transfer 9 (1995) 686.
[14] R.A. Guyer, J.A. Krumhansl, Solution of the linearized Boltzmann equation, Physical Review 148 (1966) 766.
[15] X. Zhou, K.K. Tamma, C.V.D.R. Anderson, On a new C- and F-processes heat conduction constitutive model and the associated generalized theory of dynamic thermoelasticity, Journal of Thermal Stresses 24 (2001) 531.
[16] W. Dai, R. Nassar, A finite difference method for solving the heat transport equation at the microscale, Numerical Methods Partial Differential Equations 15 (1999) 698.
[17] W. Dai, R. Nassar, A compact finite difference scheme for solving a one-dimensional heat transport equation at the micro-scale, Journal of Computational and Applied Mathematics 132 (2001) 431.
[18] W. Dai, R. Nassar, A finite difference scheme for solving a three dimensional heat transport equation in a thin film with micro-scale thickness, International Journal for Numerical Methods in Engineering 50 (2001) 1665.
[19] W. Dai, R. Nassar, An unconditionally stable finite difference scheme for solving 3-D heat transport equation in a sub-microscale thin film, Journal of Computational and Applied Mathematics 145 (2002) 247.
[20] W. Dai, R. Nassar, A compact finite difference scheme for solving a three-dimensional heat transport equation in a thin film, Numerical Methods for Partial Differential Equations 16 (2000) 441.
[21] J. Zhang, J.J. Zhao, Unconditionally stable finite difference scheme and iterative solution of 2D microscale heat transport equation, Journal of Computational Physics 170 (2001) 261.
[22] J. Zhang, J.J. Zhao, Iterative solution and finite difference approximations to 3D microscale heat transport equation, Mathematics and Computers in Simulation 57 (2001) 387.
[23] J. Douglas, J.E. Gunn, A general formulation of alternating direction methods, Numerische Mathematik 6 (1964) 428.
[24] I. Kunadian, J.M. McDonough, R.R. Kumar, An efficient numerical procedure for solving a microscale heat transport equation during femtosecond laser heating of nanoscale metal films, ASME InterPACK '05, San Francisco, CA, USA, July 17–22, 2005.
[25] R.R. Kumar, J.M. McDonough, M.P. Mengüç, I. Kunadian, Performance comparison of numerical procedures for efficiently solving a microscale heat transport equation during femtosecond laser heating of nanoscale metal films, #IMECE2005-79542, ASME IMECE '05, Orlando, FL, 2005.
[26] K.S. Chiu, Temperature-dependent Properties and Microvoid in Thermal Lagging, Ph.D. Dissertation, University of Missouri-Columbia, Columbia, MO, 1999.
[27] S.D. Brorson, A. Kazeroonian, J.S. Moodera, D.W. Face, T.K. Cheng, E.P. Ippen, M.S. Dresselhaus, G. Dresselhaus, Femtosecond room temperature measurements of the electron–phonon coupling constant λ in metallic superconductors, Physical Review Letters 64 (1990) 2172.